Preparation, Characterization and Crystal Structure of the Room Temperature Phase of $[(CH_3)(C_6H_5)_3P]_2[ZnBr_4]$: A Member of the A_2BX_4 Family

Mohga F. Mostafa[a], Ahmed A. Youssef[a], Thanaa S. El-Dean[a], Aisha M. Mostafa[b], and Ibrahim S. Farag[b]

[a] Physics Department, Faculty of Science, University of Cairo, Cairo, Egypt
[b] Solid State Department, Physics Division, National Research Centre, Dokki, Cairo, Egypt

Reprint requests to Dr. M. F. M.; E-mail: Mohga40@yahoo.com

Z. Naturforsch. **62a,** 549 – 554 (2007); received March 21, 2007

The compound bis(methyltriphenylphosphonium) tetrabromozincate(II), $[C_{19}H_{18}P]_2[ZnBr_4]$, $M_r = 939.640$, has a monoclinic unit cell, space group $P2_1$. The lattice parameters are $a = 9.7693(4)$ Å, $b = 12.5508(4)$ Å, $c = 16.5372(6)$ Å, $\alpha = 90.00°$, $\beta = 105.2670(11)°$, $\gamma = 90.00°$, $V = 1956.11(11)$ Å^3, $Z = 2$, $D_x = 1.595$ mg m^{-3} at $T = 298$ K. The structure consists of one distorted $[ZnBr_4]^{2-}$ tetrahedron and two $[(CH_3)(C_6H_5)_3P]^+$ cations. Differential scanning calorimetry indicates a continuous second-order transition at (276 ± 2) K that may be classified as a commensurate to incommensurate transformation. A first-order transition to a higher symmetry is associated with a four-fold rotation of the $[ZnBr_4]^{2-}$ ion and a change of entropy $\Delta S = 22.92$ J/(K · mol) at $T = (362 \pm 3)$ K.

Dilatometric measurements showed a decrease of the lattice parameters in the temperature range 230 – 260 K, confirmed the transition at (276 ± 2) K, and indicated the presence of a third transition at 282 K.

Key words: Crystal Structure; Phase Transition; Commensurate-Incommensurate.
PACS numbers: 61.10.i, 64.70.Kb, 61.44.Fw.

1. Introduction

Many compounds in the A_2BX_4 family, where A is a monopositive cation and BX_4 a dinegative tetrahedral anion, exhibit several structural transformations at low and high temperatures with the highest temperature phase having the β-K_2SO_4 symmetry [1]. These materials are known to undergo several successive and interesting phase changes, some of which are commensurate (C) to incommensurate (IC) transitions [2 – 7]. The $[(CH_3)_4N]_2[ZnBr_4]$ salt is known to undergo a C to IC transition at (286 ± 1) K, while $[(C_2H_5)_4N]_2[ZnBr_4]$ undergoes a second-order transition at (230 ± 1) K [8]. This shows the importance of the role played by the cation. Upon replacing the N by a P atom only one second-order transition at $T = 368.7$ K was observed in $[(CH_3)_4P]_2[ZnBr_4]$, where a structural transition from monoclinic $P2_1/c$ to high temperature orthorhombic $Pmcn$ symmetry took place, but no C-IC transition was reported [9]. However a C-IC transition was found in the corresponding copper salt [10, 11]. This means that the phase behaviour must be sensitive to changes of the cation and anion. Therefore preparation of $[(CH_3)(C_6H_5)_3P]_2[ZnBr_4]$, its characterization and structure determination as well as its phase behaviour would help to understand the nature and mechanism of phase transitions in these magnetic insulators.

2. Experimental

2.1. Sample Preparation

The sample was prepared by mixing an acidified alcoholic solution of methyltriphenylphosphonium bromide (MTPB) with an alcoholic solution of $ZnBr_2$ in the ratio 2 : 1. The solution was kept at 70 °C for 1 h. Small transparent crystals were obtained upon gradual cooling to room temperature. The product was washed with a mixture of diethyl ether and ethanol, redissolved in ethanol and kept at 32 °C for three weeks to crystallize. The obtained crystals were washed, dried and kept under vacuum.

The sample had a melting point of 170 °C. Chemical analysis revealed the formation of a material with the

0932–0784 / 07 / 0900–0549 $ 06.00 © 2007 Verlag der Zeitschrift für Naturforschung, Tübingen · http://znaturforsch.com

Compound	ν13	ν10	ν15	ν16	ν17	ν18
$[(CH_3)_4P]_2[MX_4]$	2986 – 2967 s	2914 – 2893 m	1435 – 1415 m	1308 – 1295 m	985 – 972 vs	778 – 769 m
MTPZB	3481 – 3047 m	2900 – 2581 s	1583 – 1482 vs	1324 m	1191 s – vs	610 s

Table 1. Observed absorption peaks (in cm^{-1}) and their assignment in the near IR range for $[(CH_3)_4P]_2[MX_4]$ and MTPZB.

formula $[(CH_3)(C_6H_5)_3P]_2[ZnBr_4]$, henceforth named MTPZB.

2.2. Infrared Spectroscopy

Infrared spectroscopy was performed using an FTIR1650 Perkin-Elmer spectrometer in the frequency range 200 – 4000 cm^{-1}.

2.3. Differential Thermal Scanning Measurements

Differential thermal scanning (DSC) measurements were carried out on a Shimadzu differential scanning model DSC-50 analyzer. The analyzer was calibrated with the melting transition of indium at 157 ℃. Low temperature measurements at 170 K and 400 K were performed using liquid nitrogen as coolant. Crystallized samples were ground, and thermographs were obtained at a scanning rate of 5 ℃/min for both the low and high temperature measurements. Two samples were measured, the transition temperatures of which were within acceptable error limits.

2.4. X-Ray Diffractometry

X-Ray crystallographic data were collected on an Enraf-Nonius 590 Kappa CCD single crystal diffractometer with a graphite monochromator using MoK_α radiation ($\lambda = 0.71073$ Å). The intensities were collected at room temperature using a φ-ω scan mode. The crystal to detector distance was 40 mm. The cell refinement and data reduction were carried out using Denzo and Scalepak programs [12]. The crystal structure was solved by the direct method using an SIR92 program [13] which revealed the positions of all non-hydrogen atoms, refined by the full matrix least square refinement based on F^2, using the maXus package [14]. Sort average multiscanning absorption corrections were applied to all data using the program SORTAV [15]. The temperature factors of all non-hydrogen atoms were refined anisotropically, then hydrogen atoms were introduced as a riding model with C-H = 0.96 Å and refined isotropically. The Molecular graphics were prepared using the ORTEP program [16].

Table 2. Thermodynamic parameters as obtained from DSC measuremens of MTPZB, $[(C_2H_4)_4N]_2[ZnCl_4]$, $[(CH_3)_4N]_2[ZnCl_4]$, $[(C_2H_4)_4N]_2[ZnBr_4]$, and $[(CH_3)_4N]_2[ZnBr_4]$.

Sample	Transition 1		Transition 2		Reference
	T_{c1}	ΔS	T_{c2}	ΔS	
MTPZB	362 ± 2	22.92	276.9	2.12	present work
$[(C_2H_4)_4N]_2[ZnCl_4]$			227	38.9	[6]
$[(CH_3)_4N]_2[ZnCl_4]$			286		[8]
$[(C_2H_4)_4N]_2[ZnBr_4]$			230		[8]
$[(CH_3)_4N]_2[ZnBr_4]$	368.7	9.15			[9]

3. Results and Discussion

3.1. Infrared Spectroscopy

Table 1 lists the observed absorption peaks and their assignment in the near IR range according to [17, 18]. The far IR spectrum contains strong bands at 376, 301, 271.9 and 121 cm^{-1} which are attributed to internal vibrations of $[ZnBr_4]^{2-}$ [19].

3.2. Thermal Analysis

Figure 1 shows the thermograph of MTPZB in the temperature range 303 to 373 K. A small λ-like peak at 276.9 K with a long tail on the low temperature side suggests a continuous second-order transition. Theoretically, the transition has zero entropy, however the calculated value is 2.12 J/K · mol. A second endothermic peak with a large enthalpy is initiated at the temperature $T_i = (362 \pm 3)$ K, the calcu-

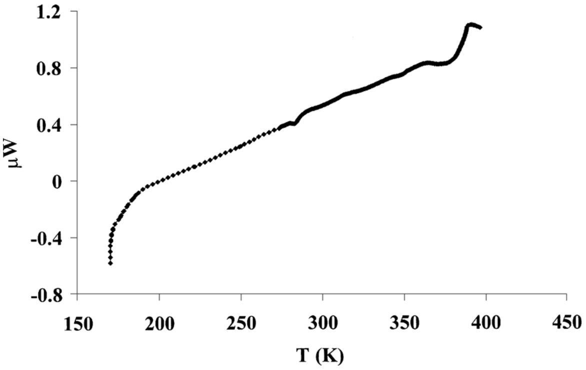

Fig. 1. Thermograph of MTPZB in the temperature range 303 – 373 K.

Table 3. X-Ray data collection parameters and refinement of MTPZB.

Chemical formula	$C_{38}H_{36}Br_4ZnP_2$
Formula mass, g mol^{-1}	939.640
Temperature, K	298
Wave length, Å	0.71073
Space group	monoclinic $P2_1$
a, Å	9.7693(4)
b, Å	12.5508(4)
c, Å	16.5372(6)
β, deg.	105.2670(11)
Volume, Å^3	1956.11(11)
Z	2
Density, mg m^{-3}	1.595
Measured reflections	5125
Independent reflections	3041
Observed reflections	2286
R_{int}	0.063
Index range	$0 \le h \le 10$, $0 \le k \le 13$, $-18 \le l \le 17$
Refining method	Full matrix least square on F^2
R Indices (all data)	$R = 0.159$, $\omega Rr = 0.105$
$\lvert\Delta/\sigma\rvert_{\text{max}}$	0.041
$\Delta\rho_{\text{fin}}$ (max / min)	0.73 / −0.74

lated entropy is $\Delta S = 22.92$ J/(K · mol). The value of a simple rotation of the $[MX_4]^{2-}$ tetrahedron about the 4-fold axis contributes 5.7 J/(K · mol), and a total disorder within the tetrahedral structure would contribute $R \ln 12 = 20.7$ J/(K · mol) to the total entropy [20]. This is in reasonable agreement with the value $\Delta S = 22.92$ J/(K · mol) obtained for the high temperature transition. Table 2 lists the transition temperatures and entropies of the presently investigated sample as well as other closely related samples.

3.3. X-Ray Structure Description

Table 4. Atomic coordinates (Å) and equivalent isotropic thermal parameters U(iso) (Å^2) of MTPZB.

	x	y	z	U_{eq}
Br1	0.78746(11)	0.75214(11)	−0.21732(8)	0.0629(7)
Br2	0.39908(13)	0.68087(11)	−0.35418(8)	0.0644(7)
Zn3	0.53966(12)	0.79980(10)	−0.24754(8)	0.0478(6)
Br4	0.45584(14)	0.77904(11)	−0.12444(8)	0.0754(8)
Br5	0.51415(17)	0.98306(11)	−0.29171(8)	0.0782(9)
P6	0.8613(3)	0.4700(2)	0.01655(19)	0.0492(16)
P7	1.0066(3)	0.4348(3)	0.43381(18)	0.0499(16)
C8	0.7894(11)	0.5838(9)	0.0570(7)	0.043(6)
C9	0.7443(11)	0.4262(10)	−0.0805(7)	0.052(7)
C10	1.1592(11)	0.3594(9)	0.4876(7)	0.047(6)
C11	0.9091(12)	0.4735(11)	0.5071(7)	0.054(7)
C19	1.0279(11)	0.5056(10)	−0.0025(9)	0.058(7)
C23	1.0632(11)	0.5533(10)	0.3888(7)	0.047(6)
C37	0.8902(13)	0.3641(11)	0.0924(8)	0.066(7)
C41	0.8994(14)	0.3525(12)	0.3524(9)	0.074(8)

Table 5. Selected bond lengths (Å) and bond angles (°) with e. s. d. in parentheses at 293 K of MTPZB.

Bond length		Bond angle	
Br1-Zn3	2.4150(7)	Br1-Zn3-Br2	109.91(3)
Br2-Zn3	2.4427(8)	Br1-Zn3-Br4	110.20(3)
Br3-Zn4	2.4007(7)	Br1-Zn3-Br5	108.46(3)
Br3-Zn5	2.4101(8)	Br2-Zn3-Br4	107.14(3)
P6-C8	1.801(4)	Br2-Zn3-Br5	111.82(3)
P6-C9	1.783(5)	Br4-Zn3-Br5	109.32(3)
P6-C10	1.791(5)	C8-P6-C9	109.3(2)
P6-C23	1.793(5)	C8-P6-C10	108.7(2)
P7-C12	1.803(5)	C8-P6-C23	109.3(2)
P7-C14	1.796(5)	C9-P6-C10	110.7(2)
P7-C16	1.826(5)	C9-P6-C23	109.6(3)
P7-C18	1.758(6)	C10-P6-C23	109.1(3)

The crystal structure data are summarized in Table 3. Table 4 lists the atomic coordinates and equivalent isotropic thermal parameters. Table 5 lists the bond distances and bond angles. The unit cell of the investigated compound consists of two crystallographically independent $(MTP)^+$ cations and the $[ZnBr_4]^{2-}$ anion, where the $(MTP)^+$ cations intercalate between the alternating tetrahedral $[ZnBr_4]^{2-}$. The cations are composed of three planar phenyl groups and one methyl group around the central phosphorus atom in the form of a distorted tetrahedron. The lengths and angles are within the accepted range. The interplay between the steric hinderance, a repulsive effect resulting from the large size of the phenyl groups, and the Van-der-Waals forces stabilizes the structure. The anions are arranged to form a cavity. Figure 2a demonstrates the arrangement of the cations and anions. The ORTEP view of the atoms is given in Figure 2b. The crystal structure describing the packing of the layers of cations indicates that the crystal structure can be regarded as a pseudo-layered structure with the two $(MTP)^+$ ions lying at nearly $y/b = 0.4$. The anion is significantly disordered, as shown by the large halide atom ellipsoids. The smaller ellipsoid of the central atom of the anion implies that the disorder, if dynamic, is primarily librational, involving rotation about the centres of mass. The bond lengths and bond angles of the two cations are slightly different, as seen in Table 5. The tetrahedral anion has bond lengths in the range between 2.3536 and 2.4036 Å and the bond angles range between 106.29 and 112.85°, which reveals their distortion. This distortion may be attributed to the steric hindrance induced by the surrounding cations.

The structure may also be compared with that of $[(CH_3)_4P]_2[ZnBr_4]$ [9], which has the same anion $[ZnBr_4]^{2-}$ but a different cation, as follows:

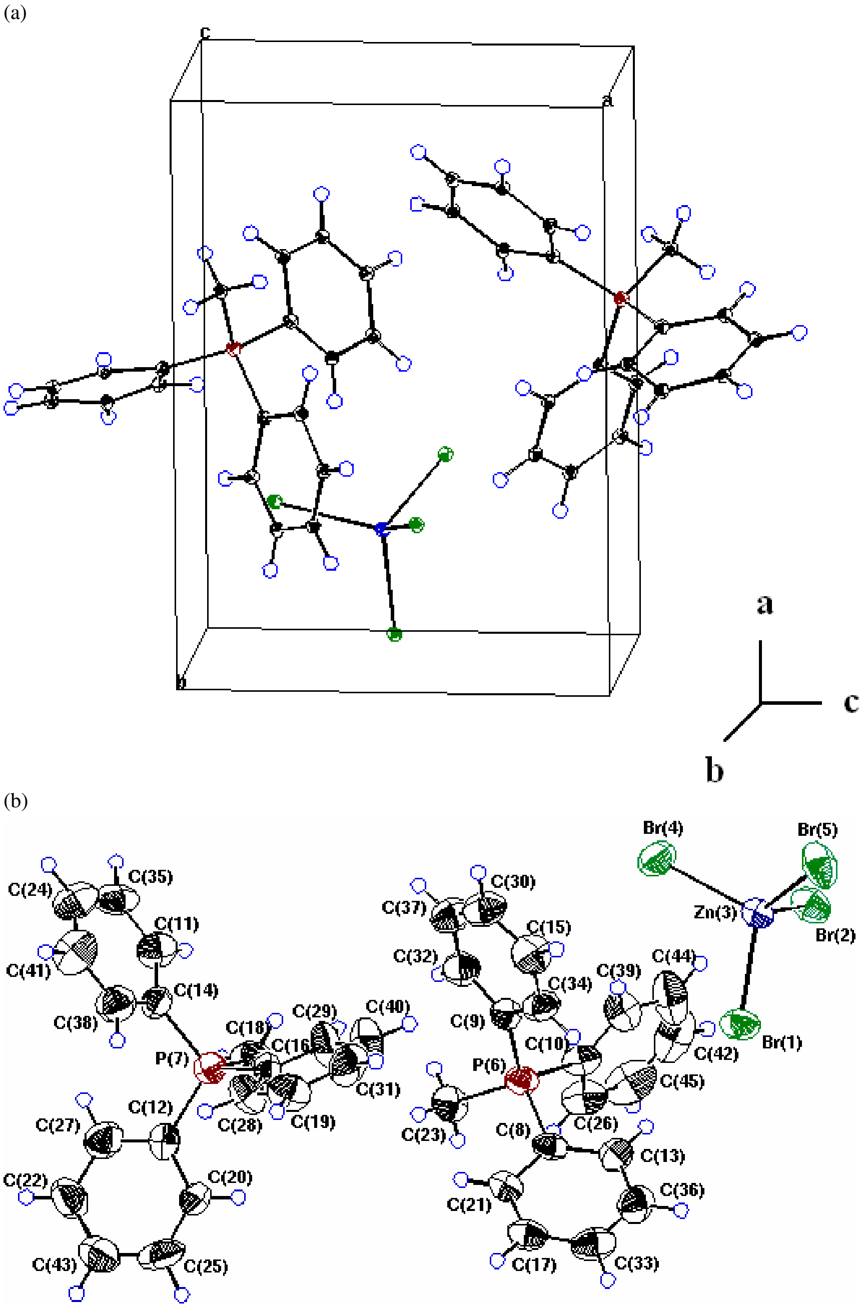

Fig. 2. (a) Structure view of MTPZB; (b) ORTEP view of the MTPZB atoms.

(i) MTPZB is monoclinic ($P2_1$), having 2 molecules per unit cell; $[(CH_3)_4P]_2[ZnBr_4]$ is monoclinic ($P2_1/c$) with 4 molecules per unit cell.

(ii) The Zn-Br average bond distance in MTPZB (2.401 – 2.443 Å) is slightly longer than that in $[(CH_3)_4P]_2[ZnBr_4]$ (2.395 – 2.416 Å). The tetrahedral bond angle is in the range 107.14(3) – 110.20(3)° for the presently studied sample compared to 107.89(8) – 112.38(8)° found in $[(CH_3)_4P]_2[ZnBr_4]$ [9], suggesting slightly less distortion of the $[ZnBr_4]^{2-}$ tetrahedron in $[(CH_3)_4P]_2[ZnBr_4]$.

(iii) The $[(CH_3)_4P]^+$ cation is expected to have a larger thermal ellipsoid compared to that of $(MTP)^+$. This is reflected in the larger isotropic displacement

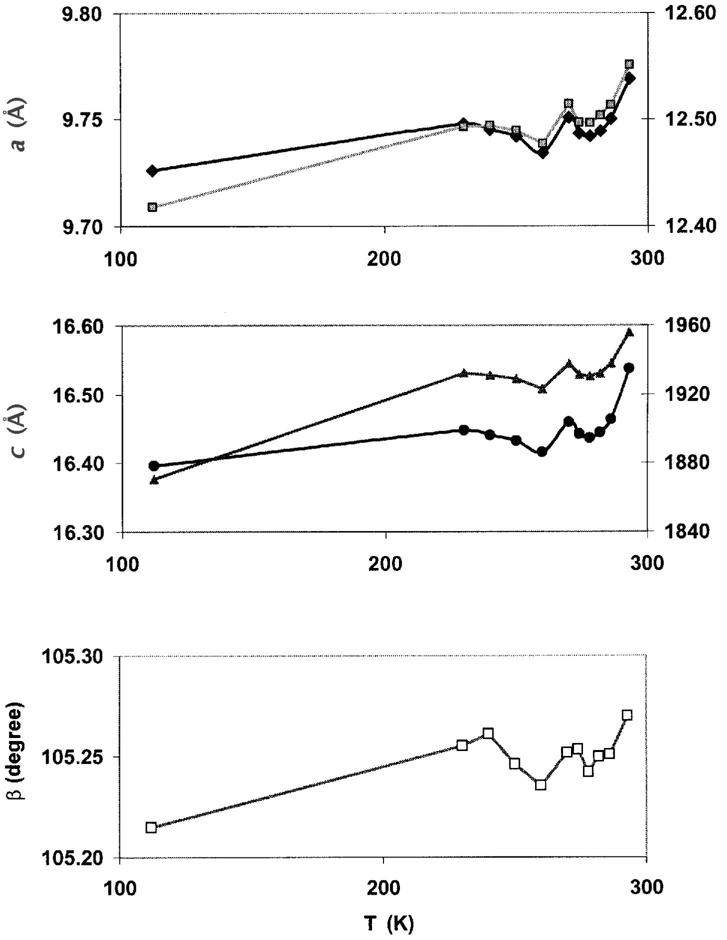

Fig. 3. Dependence of the lattice parameters on temperature.

parameters U(iso) of the $[(CH_3)_4P]^+$ cation [$U(\mathrm{iso}) \simeq 150 \cdot 10^{-3}$ Å^2] compared to $\sim 70 \cdot 10^{-3}$ Å^2 for $(MTP)^+$.

(iv) The $[(CH_3)_4P]^+$ ion has spherical geometry, while the $(MTP)^+$ ion has not.

These differences are likely to affect the phase transitions and hence the electric and magnetic properties of MTPZB.

3.4. Thermal Expansion

Generally the X-ray investigation of the anomalies in the thermal expansion agrees with anomalies in thermal analysis results. Variation of the lattice parameters with the temperature are shown in Figure 3. The DSC results and preliminary polarization measurements have indicated that there are no structural changes at temperatures below 230 K. Hence the dilatometric measurements were carried out between 230 and 295 K. The measurements were started by cooling to 100 K, and one measurement was recorded at that temperature. The sample was then heated at a rate of 10 °C/min up to 230 K, and measurements were recorded every 10 K up to 270 K (that is the range of the low temperature tail observed by the DSC thermograph). In the range $270 \text{ K} < T < 294 \text{ K}$ the data were collected every 4 K. It is clear that all lattice parameters are varying in the same manner, i. e. tending to an increase with increasing temperature except for the appearance of the two minima at 260 K and 276 K. The crystal volume also shows this behaviour. Although only one anomaly (at $T = 276$ K) was observed in the DSC thermograph, yet, preliminary measurements of the permittivity and polarization in our laboratory confirm the existence of the two anomalies at 260 K and 276 K. Details of these measurements will be published soon.

The presented DSC and X-ray investigations suggest that the material undergoes at least three structural transitions, at 260 K, (276 ± 2) K and (362 ± 3) K. In analogy with previously studied A_2BX_4 materials [2–10] we expect that the phase change at $T = (362 \pm 3)$ K will undergo a transition from its room temperature $P2_1$ phase to its high symmetry *Pmcn* phase. At low temperatures the observed continuous transformation is likely to be associated with a C to IC transition. The preliminary permittivity studies indicate anomalous changes at 260 K and 278 K, that are frequency-dependent. The results will be published shortly.

[1] M. Iizum, J. Axe, G. Shrane, and K. Shimaoka, Phys. Rev. B **15**, 4392 (1977).

[2] K. Gesi, J. Phys. Soc. Jpn. **51**, 203 (1982).

[3] R. Perret, Y. Beaucamps, G. Godefroy, P. Muralt, M. Ehrensperger, H. Arend, and D. Altermatt, J. Phys. Soc. Jpn. **52**, 2523 (1983).

[4] P. Trouelan, J. Lefebvre, and P. Derollez, Acta Cryst. C **40**, 386 (1984).

[5] P. Trouelan, J. Lefebvre, and P. Derollez, Acta Cryst. C **41**, 846 (1985).

[6] A. Wolthius, W. J. Huiskamp, L. J. De Jongh, and R. Carlin, Physica B **142**, 301 (1986).

[7] T. Asahi, K. Hasebe, and K. Gesi, J. Phys. Soc. Jpn. **57**, 219 (1988).

[8] M. Kahrizi, S. Misra, J. Kotlinski, M. Steinitz, and T. S. Plamer, Solid State Commun. **79**, 167 (1991).

[9] S. Jerebets, M. Zou, and R. D. Willett, J. Phys. Chem. Solids **63**, 793 (2002).

[10] G. Madariaga, M. M. Alberdi, and F. J. Zuniga, Acta Cryst. C **46**, 2363 (1990).

[11] P. Saint-Gregoire, R. Almairac, A. Astito, J. Lapasset, and J. Moret, Solid State Commun. **80**, 451 (1991).

[12] Z. Otwinowski and W. Minor, Processing of X-Ray Diffraction Data Collected in Oscillation Mode, in: Macromolecular Crystallography, Part A (Eds. C. W. Carter, Jr. and R. M. Sweet), Academic Press, New York 1997.

[13] A. Altomar, G. Cascarano, C. Giacovazzo, A. Guagliardi, M. C. Burla, G. Polidori, and M. Camalli, J. Appl. Cryst. **27**, 435 (1994).

[14] S. Mackay, C. J. Gilmore, C. Edwards, N. Stewart, and K. Shankland, maXus Computer Program for the Solution and Refinement of Crystal Structures, Bruker Nonius, The Netherlands, MacScience, Japan and The University of Glasgow, UK 1999.

[15] R. H. Blessing, Acta Cryst. A **51**, 33 (1995).

[16] C. K. Johnson, ORTEP–II. A Fortran Thermal-Ellipsoid Plot Program, Report ORNL-5138, Oak Ridge National Laboratory, Oak Ridge, Tennessee, USA 1976.

[17] R. W. Berg, Spetrochim. Acta **34A**, 655 (1978).

[18] G. Tatzel, H. Schrem, and J. Weidlein, Spetrochim. Acta **34** A, 549 (1978).

[19] S. Kaarup and R. Berg, Solid State Chem. **26**, 59 (1978).

[20] T. P. Melia and R. Merrifeld, J. Chem. Soc. A, 1258 (1971).